

# Killed but metabolically active microbes: a new vaccine paradigm for eliciting effector T-cell responses and protective immunity

D G Brockstedt<sup>1,5</sup>, K S Bahjat<sup>1,5</sup>, M A Giedlin<sup>1,5</sup>, W Liu<sup>1</sup>, M Leong<sup>1</sup>, W Lockett<sup>1</sup>, Y Gao<sup>1</sup>, P Schnupf<sup>2</sup>, D Kapadia<sup>1</sup>, G Castro<sup>1</sup>, J Y H Lim<sup>1</sup>, A Sampson-Johannes<sup>1</sup>, A A Herskovits<sup>2</sup>, A Stassinopoulos<sup>1</sup>, H G Archie Bouwer<sup>2</sup>, J E Hearst<sup>1</sup>, D A Portnoy<sup>2,4</sup>, D N Cook<sup>1</sup> & T W Dubensky, Jr.<sup>1</sup>

**We developed a new class of vaccines, based on killed but metabolically active (KBMA) bacteria, that simultaneously takes advantage of the potency of live vaccines and the safety of killed vaccines. We removed genes required for nucleotide excision repair (*uvrAB*), rendering microbial-based vaccines exquisitely sensitive to photochemical inactivation with psoralen and long-wavelength ultraviolet light. Colony formation of the nucleotide excision repair mutants was blocked by infrequent, randomly distributed psoralen crosslinks, but the bacterial population was able to express its genes, synthesize and secrete proteins. Using the intracellular pathogen *Listeria monocytogenes* as a model platform, recombinant psoralen-inactivated *Lm*  $\Delta$ *uvrAB* vaccines induced potent CD4<sup>+</sup> and CD8<sup>+</sup> T-cell responses and protected mice against virus challenge in an infectious disease model and provided therapeutic benefit in a mouse cancer model. Microbial KBMA vaccines used either as a recombinant vaccine platform or as a modified form of the pathogen itself may have broad use for the treatment of infectious disease and cancer.**

A major challenge for the international biomedical community is to develop vaccines for chronic diseases caused by intracellular pathogens. AIDS, malaria, tuberculosis and hepatitis are all established through chronic intracellular infections, and protection against the pathogens causing these diseases requires vaccines that elicit broad cellular immunity<sup>1</sup>. Vaccines based on either recombinant proteins or killed whole pathogens, although safe, typically induce weak cellular immunity. In contrast, vaccines based on live attenuated forms of a pathogen may have enhanced immunogenicity and elicit responses of increased breadth and durability, but they present safety risks, particularly among immunocompromised individuals. To address this dilemma in vaccine development, we sought to derive vaccine platforms based on whole organisms that elicited strong cellular immunity, yet retained the safety profile of killed or subunit vaccines.

Killed but metabolically active (KBMA) vaccines are based on bacterial nucleotide excision repair mutants, and are inactivated by photochemical treatment with a synthetic highly reactive psoralen known as S-59. Psoralens form covalent monoadducts and crosslinks with pyrimidine bases of DNA and RNA upon illumination with long-wavelength ultraviolet (UVA) light<sup>2</sup>. The primary repair pathway for psoralen crosslinks is nucleotide excision repair<sup>3</sup>, a process initiated by the ABC excinuclease, a nuclease encoded by the ultraviolet light response (*uvr*) genes. Deletion of any one of the three *uvr* genes renders bacteria exquisitely sensitive to

ultraviolet light-induced DNA damage and to psoralen-induced crosslinks<sup>3</sup>. The KBMA vaccine approach is based on the hypothesis that the increased sensitivity of *uvr* mutant strains to photochemical inactivation is correlated with randomly distributed, infrequent psoralen crosslinks, leaving intact the ability of a population of inactivated bacteria to express its genes, while preventing productive growth and the ability to cause disease in the immunized host. Thus, the early events in the natural infection are unaffected, which facilitates the induction of an innate and adaptive immune response comparable to that induced by the live pathogen.

We used *Listeria monocytogenes* as a model intracellular pathogen to test this vaccine concept. *L. monocytogenes* is a Gram-positive facultative intracellular pathogen of animals and humans that has been studied for decades as a model to understand basic aspects of cellular immunology and microbial pathogenesis<sup>4–6</sup>. *L. monocytogenes* is a powerful inducer of innate immunity as it encounters cellular effectors, resulting in the release of T helper type 1 (T<sub>H</sub>1) polarizing cytokines<sup>6</sup>. *L. monocytogenes* taken up by macrophages and dendritic cells (DCs) escape the phagolysosome and access the cytosol in a process mediated by listeriolysin O (LLO)<sup>7,8</sup>. In response to entry of bacteria into the cytosol, infected host cells produce interferon (IFN)- $\beta$ <sup>9</sup>, which, in contrast to viruses, may augment the pathogenicity of *L. monocytogenes*<sup>10–12</sup>. In the mouse listeriosis model, the liver and spleen are the primary targets of infection<sup>4</sup>. Within these target organs, bacteria spread intercellularly and remain

<sup>1</sup>Cerus Corporation, 2411 Stanwell Drive, Concord, California 94520, USA. <sup>2</sup>Department of Molecular and Cell Biology, Oregon Health Sciences University, 3710 SW US Veterans Hospital Road, Portland, Oregon 97201, USA. <sup>3</sup>Veterans Affairs Medical Center, Department of Molecular Microbiology and Immunology, Oregon Health Sciences University, 3710 SW US Veterans Hospital Road, Portland, Oregon 97201, USA. <sup>4</sup>School of Public Health, University of California, 508 Barker Hall, #3202, Berkeley, California, 94720-3202, USA. <sup>5</sup>These authors contributed equally to this work. Correspondence should be addressed to T.W.D. (tom\_dubensky@cerus.com).

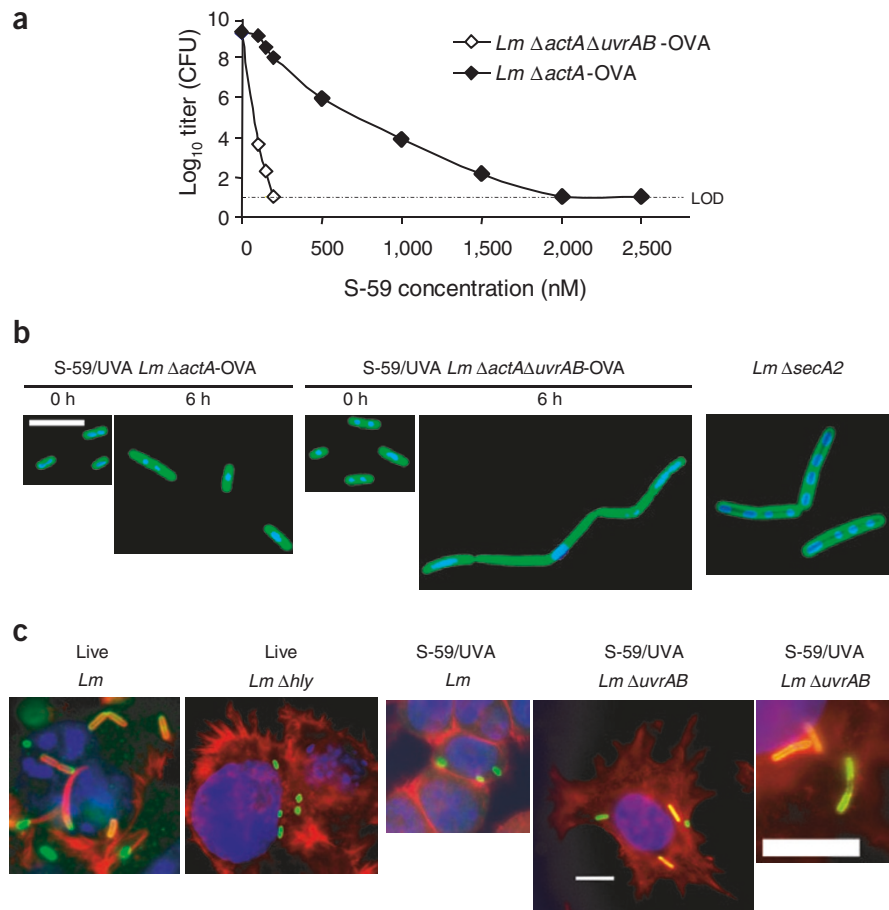


**Figure 1** *L. monocytogenes* nucleotide excision repair mutants are exquisitely sensitive to photochemical inactivation and are metabolically active. **(a)** Viability of *Lm*  $\Delta actA$ -OVA and *Lm*  $\Delta actA\Delta uvrAB$ -OVA after treatment with the indicated S-59 concentration. A representative of at least five experiments is shown.

**(b)** Immunofluorescence photomicrographs show that S-59-inactivated nucleotide excision repair mutant vaccine strains are metabolically active and form chains after incubation in broth culture; *L. monocytogenes* (green) and chromosomal DNA (blue). A *Lm*  $\Delta secA2$  mutant strain is shown for comparison and shows productive *L. monocytogenes* vegetative growth with chromosome segregation (right). The *Lm*  $\Delta secA2$  mutant strain grows in chains due to lack of secretion of peptidoglycan autolysins<sup>46</sup>. **(c)** Immunofluorescence photomicrographs show that psoralen-inactivated *Lm*  $\Delta actA\Delta uvrAB$ -OVA escape from the phagolysosome of infected DC2.4 cells. Cytosolic *L. monocytogenes* is indicated by colocalization of bacteria (green) with actin (red); host-cell DNA (blue). Scale bar, 10  $\mu$ m. Representative fields are shown.

of S-59 psoralen concentrations, using conditions established previously for Gram-positive bacteria<sup>2</sup>. The lowest S-59 concentration that resulted in full inactivation of the culture was established for each bacterial strain. *Lm*  $\Delta actA\Delta uvrAB$ -OVA was  $\geq 8$  logs more sensitive at low S-59 concentration to photochemical inactivation than parental *Lm*  $\Delta actA$ -OVA (**Fig. 1a**). We also constructed a

largely sequestered from the extracellular milieu. Acquired immunity is entirely cell mediated, and antibodies have no role in protection<sup>6</sup>.

A well-known dichotomy in the mouse listeriosis model is that, whereas wild-type *L. monocytogenes* primes potent effector and memory T-cell responses that protect mice against bacterial challenge, vaccination with LLO-deleted *L. monocytogenes* (*Lm*  $\Delta hly$ ) or with heat-killed *L. monocytogenes* does not elicit functional T cells or induce protective immunity<sup>13</sup>. This difference is evidence of the requirement for *de novo* gene expression and cytosolic access upon uptake of *L. monocytogenes* by host cells in vaccinated animals. Here, we show that psoralen-inactivated *L. monocytogenes* nucleotide excision repair mutants (*Lm*  $\Delta uvrAB$ ) retained essential properties of live bacteria, and as a result elicited functional T cells and long-term protective immunity in vaccinated mice that correlated with efficacy in mouse models of infectious disease and cancer.

## RESULTS

### *Lm* $\Delta uvrAB$ psoralen inactivation and metabolic activity

The ActA protein (encoded by *actA*) is required for cell-to-cell spread of *L. monocytogenes*<sup>8</sup>. Although live *Lm*  $\Delta actA$  mutants are attenuated 1,000-fold in mouse virulence, the potency of vaccines derived from this strain is not affected<sup>14</sup>. We constructed nucleotide excision repair mutants by removing the *uvrAB* genes in attenuated *L. monocytogenes*-based vaccines in which *actA* was deleted and which encoded the chicken ovalbumin (OVA) model antigen (*Lm*  $\Delta actA\Delta uvrAB$ -OVA). We determined the relative sensitivity to photochemical inactivation of *Lm*  $\Delta actA\Delta uvrAB$ -OVA and its parental *Lm*  $\Delta actA$ -OVA strain over a range

nucleotide excision repair mutant strain of *B. anthracis* (Sterne) by deleting *uvrAB* genes through allelic exchange (*Ba*  $\Delta uvrAB$ ). *Ba*  $\Delta uvrAB$  was  $\geq 8$  logs more sensitive to photochemical inactivation at 50 nM S-59 as compared to its parental strain (**Supplementary Fig. 1** online). We measured the number of residual viable bacteria after treating 14 individual cultures ( $\sim 10^{11}$  colony-forming units (CFU)) of *Lm*  $\Delta actA\Delta uvrAB$ -OVA and *Lm*  $\Delta actA$ -OVA. On average, 1 colony ( $\pm 3$ ) grew from *Lm*  $\Delta actA\Delta uvrAB$ -OVA cultures treated with 200 nM S-59, and 56 colonies ( $\pm 61$ ) grew from cultures of parental *Lm*  $\Delta actA$ -OVA treated with 2,500 nM S-59, indicating incomplete killing of the DNA repair-competent parental strain despite using 12.5 times more psoralen. These S-59 concentrations were the standard photochemical inactivation conditions used for subsequent experiments, and therefore resulted in at least 10-log inactivation of *Lm*  $\Delta actA\Delta uvrAB$ -OVA cultures, and approximately 9-log inactivation of cultures of the parental *Lm*  $\Delta actA$ -OVA strain with intact nucleotide excision repair.

Next, we directly measured the psoralen adduct frequency in the DNA genomes of photochemically treated vaccines over a concentration range of <sup>14</sup>C-labeled S-59 (**Table 1**). Under the standard S-59 psoralen/UVA light photochemical inactivation (S-59/UVA) conditions, *Lm*  $\Delta actA\Delta uvrAB$ -OVA genomes had a significantly lower frequency of psoralen adducts compared to parental strain genomes, *Lm*  $\Delta actA$ -OVA ( $28 \pm 5$  versus  $178 \pm 6$  psoralen adducts/*L. monocytogenes* genome, respectively;  $P = 0.00075$ ). Metabolic labeling showed substantial levels of new protein synthesis and secretion after photochemical inactivation from S-59/UVA *Lm*  $\Delta actA\Delta uvrAB$ -OVA, but not from S-59/UVA *Lm*  $\Delta actA$ -OVA (**Supplementary Fig. 2** online). The observed differences

in the level of protein synthesis between S-59/UVA *Lm*  $\Delta$ actA/ $\Delta$ uvrAB-OVA and live cultures may reflect a stress response<sup>15</sup> to photochemical treatment. Consistent with the observation of continued metabolic activity after photochemical treatment, S-59/UVA *Lm*  $\Delta$ actA/ $\Delta$ uvrAB-OVA, but not S-59/UVA *Lm*  $\Delta$ actA-OVA, formed filamentous chains upon incubation in brain-heart infusion broth after photochemical treatment, indicative of cell-wall synthesis without the ability to septate (Fig. 1b).

We next sought to determine whether this differential metabolic activity could be observed during infection of cultured cells. Expression of LLO is essential for escape of *L. monocytogenes* from the phagolysosome of the infected host cell, and entry into the cytosol is a requisite step for induction of protective immunity in vaccinated mice<sup>6,8,16</sup>. We assessed the capacity for S-59/UVA *Lm*  $\Delta$ uvrAB to escape from the phagolysosome of infected DC 2.4 cells, a mouse dendritic cell line<sup>17</sup>, by fluorescence microscopy. We measured the frequency of cytosolic *L. monocytogenes* by colocalization of bacteria with host-cell actin. A single *L. monocytogenes* protein, ActA, mediates the polymerization of host actin filaments on the bacterial cell surface, a necessary step for cytosolic motility<sup>8</sup>. All *L. monocytogenes* strains used for fluorescence microscopy contained native *actA*, in order to visualize cytosolic access by phytochemically treated bacteria through colocalization with polymerized host-cell actin. At 5 h after infection, S-59/UVA *Lm*  $\Delta$ uvrAB, but not S-59/UVA wild-type *L. monocytogenes*, formed multiple short bacteria chains that were enshrouded by host-cell actin, indicating that the S-59/UVA nucleotide excision repair mutants accessed the host-cell cytosol (Fig. 1c). Unlike live *Lm*  $\Delta$ uvrAB, S-59/UVA *Lm*  $\Delta$ uvrAB were not able to septate

**Table 1** Psoralen adduct frequency in S-59/UVA-treated *L. monocytogenes* strains

<i>Lm</i> $\Delta$ actA-OVA			<i>Lm</i> $\Delta$ actA/ $\Delta$ inlB-OVA		
[S-59] (nM)	Adducts/ genome	bp/adduct	[S-59] (nM)	Adducts/ genome	bp/adduct
0	0	N/A	0	0.5	7,028,459
100	6.5	555,940	100	12.5	287,926
200	19.3	186,098	200 <sup>a</sup>	28.1	127,968
300	19.3	186,633	300	53.0	67,925
400	19.3	186,110	400	110.5	32,570
1,200	74.1	48,610	1,200	495.9	7,260
2,500 <sup>a</sup>	177.8	20,253	2,500	637.6	5,646

<sup>a</sup>Conditions for each strain that resulted in complete inactivation as determined by the inability to form colonies overnight on brain-heart infusion agar plates.

and did not form the signature ‘comet tail’ indicative of cytosolic motility<sup>18</sup>. Quantitative fluorescence microscopy of cytosolic *L. monocytogenes* 5 h after infection showed that 61% of live bacteria (521 of 855) and 47% of S-59/UVA *Lm*  $\Delta$ uvrAB (493 of 1,047), respectively, escaped the phagolysosome (combined data from five individual experiments; data not shown). In contrast, we detected less than 5% of S-59/UVA wild-type *Lm* or *Lm*  $\Delta$ hly (LLO<sup>-</sup>) in the cytosol (Fig. 1c).

The host cell recognizes bacterial products in the cytosol, leading to production of IFN- $\beta$ . Synthesis of IFN- $\beta$  distinguishes between bacteria confined to the vacuole and bacteria that can propagate in the cytosol. Rapid induction of mRNA encoding IFN- $\beta$  was observed in primary C57BL/6 mouse bone marrow-derived macrophages infected with both live *L. monocytogenes* strains and with S-59/UVA *Lm*  $\Delta$ actA/ $\Delta$ uvrAB-OVA. As shown previously<sup>9</sup>, we did not observe induction of mRNA encoding IFN- $\beta$  in macrophages infected with live *Lm*  $\Delta$ hly. Together, these data show that nucleotide excision repair mutant vaccines are exquisitely sensitive to psoralen-mediated photochemical inactivation and contain a significantly ( $P = 0.00075$ ) reduced frequency of adducts

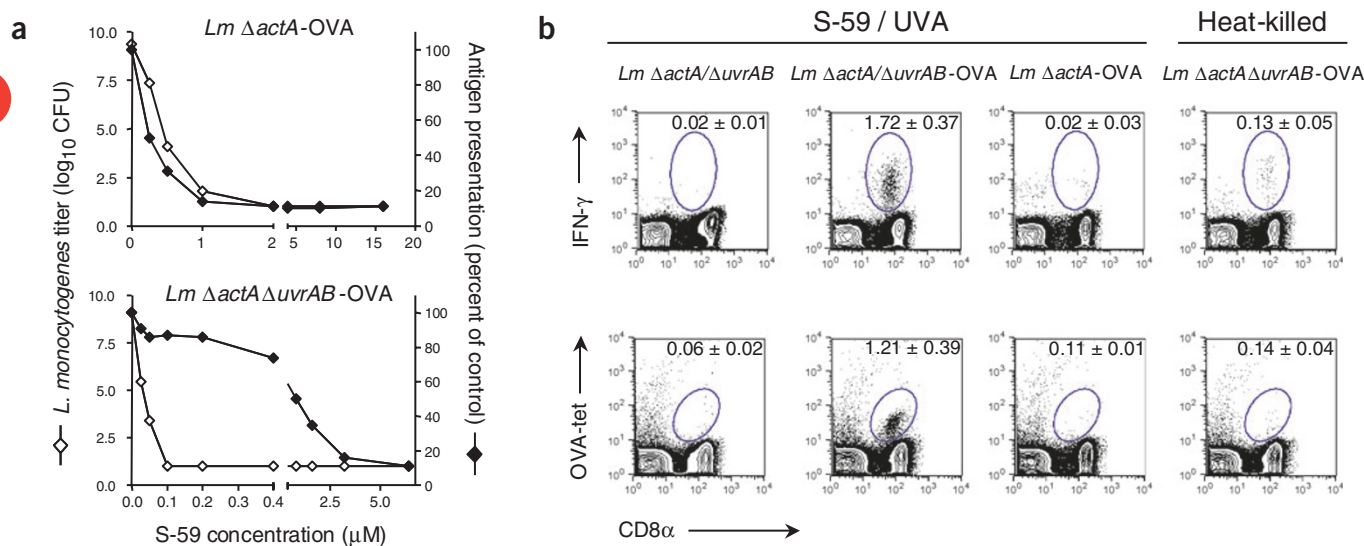


**Figure 2** Photochemically inactivated *L. monocytogenes* nucleotide excision repair mutant vaccines induce class I responses. **(a)** S-59/UVA *Lm*  $\Delta$ actA/ $\Delta$ uvrAB-OVA load antigen into the MHC class I pathway of antigen-presenting cells. DC2.4 cells were infected with *L. monocytogenes* vaccines treated with varying concentrations of S-59 psoralen as indicated and illuminated with 6 J/cm<sup>2</sup> UVA light. H-2K<sup>b</sup>-restricted presentation of SIINFEKL epitope measured by B3Z activation (filled diamond; represented as percent of live bacteria) as a function of *L. monocytogenes* viability (open diamond) is shown. A representative of at least three experiments is shown. **(b)** Bone marrow-derived DCs infected with S-59/UVA *Lm*  $\Delta$ actA/ $\Delta$ uvrAB-OVA prime functional CD8<sup>+</sup> T cells in mice. Splenic OVA-specific CD8<sup>+</sup> T cells were measured by TNF- $\alpha$  and IFN- $\gamma$  cytokine flow cytometry and tetramer analysis. Data are presented as mean  $\pm$  s.d. Representative dot plots for three mice per group are shown. This experiment was repeated twice with similar results.

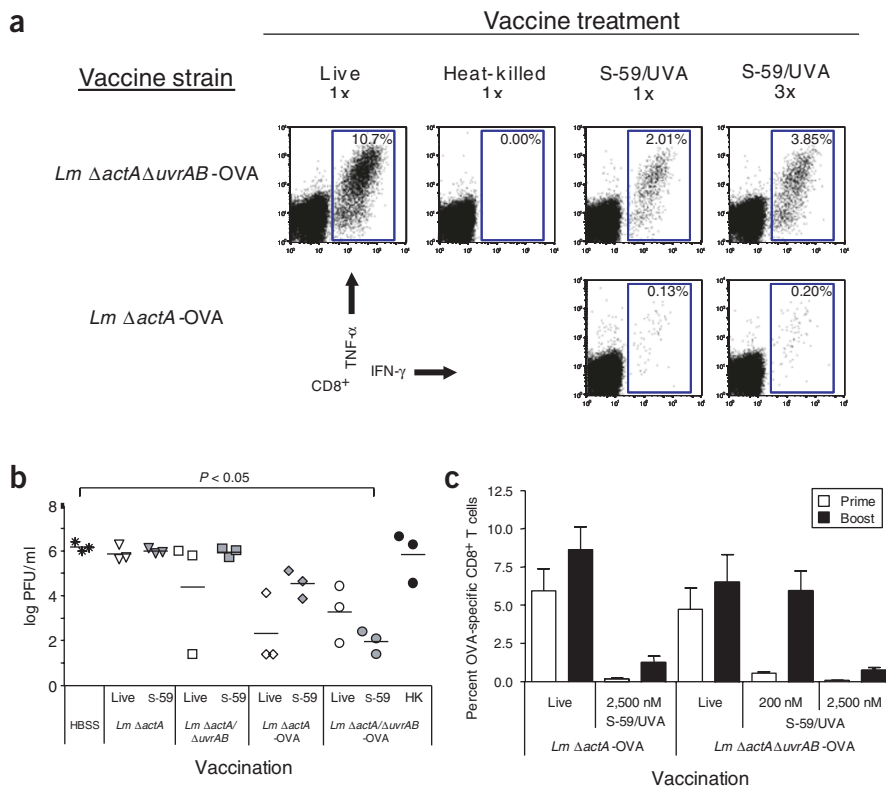


**Figure 3** S-59/UVA *Lm ΔactA/ΔuvrAB-OVA* elicit functional CD8<sup>+</sup> T cells in vaccinated mice and protect against a subsequent viral challenge. **(a)** OVA-specific CD8<sup>+</sup> T-cell responses determined 1 week after immunization. **(b)** Protection against rVV-OVA challenge. One-way ANOVA,  $P = 0.0273$ ; Kruskal-Wallis nonparametric test with Dunn post test. HK, heat-killed. **(c)** Primary T-cell responses induced by S-59/UVA *Lm ΔactA/ΔuvrAB-OVA* can be boosted. Primary OVA-specific CD8<sup>+</sup> T-cell responses were determined 7 d after immunization with the indicated strains. The secondary T-cell response was determined 6 d after boost immunization on day 14. Data are presented as mean  $\pm$  s.e.m. All data represent at least three independent experiments.

in the genome; thus, a larger proportion of the genome is available for transcription. S-59/UVA *Lm ΔactA/ΔuvrAB-OVA*, although unable to grow productively, retains sufficient metabolic activity to access the cytosol of infected cells, a necessary step for induction of CD8<sup>+</sup> T cells and protective immunity.

### S-59/UVA *Lm ΔuvrAB* MHC class I antigen presentation

Proteins secreted from viable cytosolic *L. monocytogenes* can be efficiently processed by the major histocompatibility complex (MHC) class I pathway<sup>19</sup>. Using OVA-specific CD8<sup>+</sup> T-cell hybridoma cells (B3Z), we determined the relative capacity of psoralen-inactivated *Lm ΔactA/ΔuvrAB-OVA* to directly load the immunodominant MHC class I OVA epitope SIINFEKL on H-2K<sup>b</sup> within infected DC2.4 cells. Notably, S-59/UVA *Lm ΔactA/ΔuvrAB-OVA*, but not parental S-59/UVA *Lm ΔactA-OVA*, maintained its capacity to load antigen into the MHC class I pathway independent of its ability to form colonies on agar media (Fig. 2a). There was a window defined by an S-59 psoralen concentration range between 100 and 400 nM in which activation of the T-cell hybridoma was not correlated with ability of S-59/UVA *Lm ΔactA/ΔuvrAB-OVA* to form colonies on agar media. In contrast, MHC class I presentation could not be unlinked from bacterial growth using the *Lm ΔactA-OVA* parental strain.

Next, we tested whether autologous immature bone marrow-derived DCs infected *ex vivo* with S-59/UVA *Lm ΔactA/ΔuvrAB-OVA* could prime functional OVA-specific CD8<sup>+</sup> T cells in vaccinated mice. We

observed functional cytokine-secreting OVA-specific CD8<sup>+</sup> T-cell responses measured 1 week after vaccination only in mice immunized with S-59/UVA *Lm ΔactA/ΔuvrAB-OVA*-infected DCs, resulting in about 2% OVA-specific CD8<sup>+</sup> T cells (Fig. 2b). In contrast, we did not observe significant CD8<sup>+</sup> T cell responses in mice vaccinated with DCs infected with either heat-killed *Lm ΔactA/ΔuvrAB-OVA* or parental S-59/UVA *Lm ΔactA-OVA*.

### S-59/UVA *Lm ΔuvrAB* protects against viral challenge

Live attenuated recombinant *L. monocytogenes* vaccines induce robust CD8<sup>+</sup> T-cell responses specific for a secreted heterologous antigen, conferring preventative or therapeutic immunity in animal models of infectious disease and cancer<sup>20,21</sup>. We immunized C57BL/6 mice with selected S-59/UVA *Lm-OVA* vaccines to determine whether abrogation of nucleotide excision repair was also required to prime CD8<sup>+</sup> T cells *in vivo* (Fig. 3a). A single vaccination with S-59/UVA *Lm ΔactA/ΔuvrAB-OVA* induced 2% OVA-specific CD8<sup>+</sup> T cells and three immunizations given on 3 consecutive days induced 3.8% OVA-specific CD8<sup>+</sup> T cells. In contrast, vaccination with S-59/UVA *Lm ΔactA-OVA* or heat-killed *Lm ΔactA/ΔuvrAB-OVA* did not result in any significant induction of OVA-specific CD8<sup>+</sup> T cells, regardless of immunization regimen. These CD8<sup>+</sup> T-cell responses correlated with protection against challenge with recombinant vaccinia virus-OVA (rVV-OVA) in mice immunized with S-59/UVA *Lm ΔactA/ΔuvrAB-OVA* (Fig. 3b). We observed a 4-log reduction in

rVV-OVA titer in the ovaries of challenged mice immunized with S-59/UVA *Lm ΔactA/ΔuvrAB-OVA*, as compared to challenged naive mice. In contrast, we observed only a 1-log reduction in virus titer in mice immunized with the S-59/UVA *Lm ΔactA-OVA* parent strain. The level of protective immunity against vaccinia challenge was not significantly different between mice immunized with S-59/UVA *Lm ΔactA/ΔuvrAB-OVA* or with live *Lm ΔactA/ΔuvrAB-OVA*.

We then evaluated the comparative immunogenicity of S-59/UVA *Lm-OVA* vaccines after a conventional prime and boost immunization dosing regimen (Fig. 3c). S-59/UVA *Lm ΔactA/ΔuvrAB-OVA*, but not S-59/UVA *Lm ΔactA-OVA*, elicited a robust OVA-specific CD8<sup>+</sup> T cells with a prime-boost immunization regimen separated by 14 d. The primary and secondary OVA-specific CD8<sup>+</sup> T-cell responses of live *Lm ΔactA/ΔuvrAB-OVA* and live *Lm ΔactA-OVA* were comparable, showing that deletion of the *uvrAB* genes does not affect the potency of live *L. monocytogenes* vaccines. The data also show that the boosted OVA-specific CD8<sup>+</sup> T-cell responses in mice immunized with live or S-59/UVA *Lm ΔactA/ΔuvrAB-OVA* vaccines were similar.

### S-59/UVA *Lm ΔuvrAB* therapeutic antitumor efficacy

We evaluated the potency of the S-59/UVA *Lm ΔuvrAB* platform in a rigorous setting of CT-26 tumor-bearing mice. Therapeutic efficacy in this model requires breaking of self-tolerance to the H-2L<sup>d</sup> immunodominant epitope AH1 from the gp70 endogenous tumor

antigen<sup>22,23</sup>. We constructed isogenic vaccines that differed only in nucleotide excision repair capacity and that expressed and secreted the altered CD8<sup>+</sup> T-cell epitope AH1-A5 (ref. 22). Therapeutic vaccination of mice with S-59/UVA *Lm ΔactA/ΔuvrAB*-AH1-A5 given on 3 consecutive days, 3 d after intravenous implantation of CT-26 tumor cells, resulted in reduction of lung tumor burden (Fig. 4a) that correlated with a significant prolongation of life (Fig. 4b). Therapeutic antitumor efficacy resulted from breaking tumor antigen self-tolerance as shown by the induction of cytolytic AH1 epitope-specific CD8<sup>+</sup> T cells *in vivo* (Supplementary Fig. 3 and Supplementary Methods online). In contrast, immunization of tumor-bearing mice with S-59/UVA parental *Lm ΔactA*-AH1-A5 did not elicit significant AH1-specific CD8<sup>+</sup> T cells or provide therapeutic benefit.

### S-59/UVA *LM ΔuvrAB* protects against bacterial challenge

To test the possibility of using S-59/UVA nucleotide excision repair mutants of pathogens as a vaccine against the cognate wild-type virulent organism, we assessed the protective immunity elicited in mice vaccinated with S-59/UVA *Lm ΔactA/ΔuvrAB*, S-59/UVA *Lm ΔactA/ΔuvrAB*, but not heat-killed *Lm ΔuvrAB* or S-59/UVA *Lm ΔactA*, induced a potent LLO<sub>190–201</sub>-specific CD4<sup>+</sup> T-cell response (Fig. 5a). We evaluated protective immunity by challenging C57BL/6 mice with twice the lethal dose in 50% of subjects (LD<sub>50</sub>) dose of wild-type *L. monocytogenes* 90 d after a prime and boost immunization regimen. We enumerated bacteria in the spleen 3 d after wild-type *L. monocytogenes* challenge. We observed comparable protective immunity—as shown by an approximate 6-log reduction in spleen colonization after wild-type *L. monocytogenes* challenge relative to control vaccinated mice—in mice vaccinated with live or S-59/UVA *Lm ΔactA/ΔuvrAB* (Fig. 5b). Notably, *Lm ΔactA/ΔuvrAB* inactivated with 2,500 nM S-59, the psoralen concentration required to inactivate the parental *Lm ΔactA* strain, did not confer protection in vaccinated mice. As expected<sup>16,24</sup>, protective immunity was not induced when mice were vaccinated with either heat-killed *Lm ΔactA/ΔuvrAB* or *Lm Δhly* (Fig. 5b). Together, these data show that S-59/UVA *Lm ΔactA/ΔuvrAB*-based vaccines retain the biologic properties of live *Lm ΔactA/ΔuvrAB* vaccines at a level sufficient to elicit protection against lethal wild-type bacterial challenge.

### DISCUSSION

We describe proof-of-concept studies for a new class of vaccines, termed 'killed but metabolically active', or KBMA, that is based on photochemically inactivated nucleotide excision repair mutant microbes. KBMA vaccines have two separate potential applications: (i) recombinant *L. monocytogenes* expressing heterologous antigens relevant to infectious disease or cancer; and (ii) vaccines for bacterial diseases based on a modified form of the pathogen itself. This latter case is theoretically advantageous in instances where the antigenic correlates of immune protection are unknown or poorly defined, such as for *Mycobacterium*

*tuberculosis*. KBMA vaccines retain the biologic properties of the parental organism, and thus stimulate relevant innate and adaptive immune responses. KBMA vaccines cannot grow productively and do not present the infectious risk inherent in live vaccines.

Deletion of nucleotide excision repair should, in principle, make a single psoralen crosslink a lethal event to a bacterium by forming an absolute block to chromosome replication. Quantitative assessment of psoralen adduct frequency supports this hypothesis. According to the Poisson distribution, an average frequency of 23 crosslinks per genome ( $3 \times 10^6$  bp), or one crosslink per 130,000 bp, would be required to kill 10 logs of *L. monocytogenes*, assuming that a single psoralen crosslink is a lethal event. The average number of psoralen adducts per genome required to inactivate 10 logs of the nucleotide excision repair mutant *Lm ΔuvrAB* was 28, approximately one psoralen adduct for every 107,000 bp, or about every 100 genes, considerably close to the frequency predicted by Poisson distribution. In contrast, the number of adducts per genome to inactivate 9 logs of its parental strain was 178, corresponding to a psoralen adduct every 17,000 bp, or about every 17 genes. Moreover, our psoralen assay measures both crosslinks and monoadducts, and thus the number of crosslinks may be less than 28 per genome. These data also suggest that deletion of nucleotide excision repair by itself is sufficient, and that deletion of *recA* or other DNA

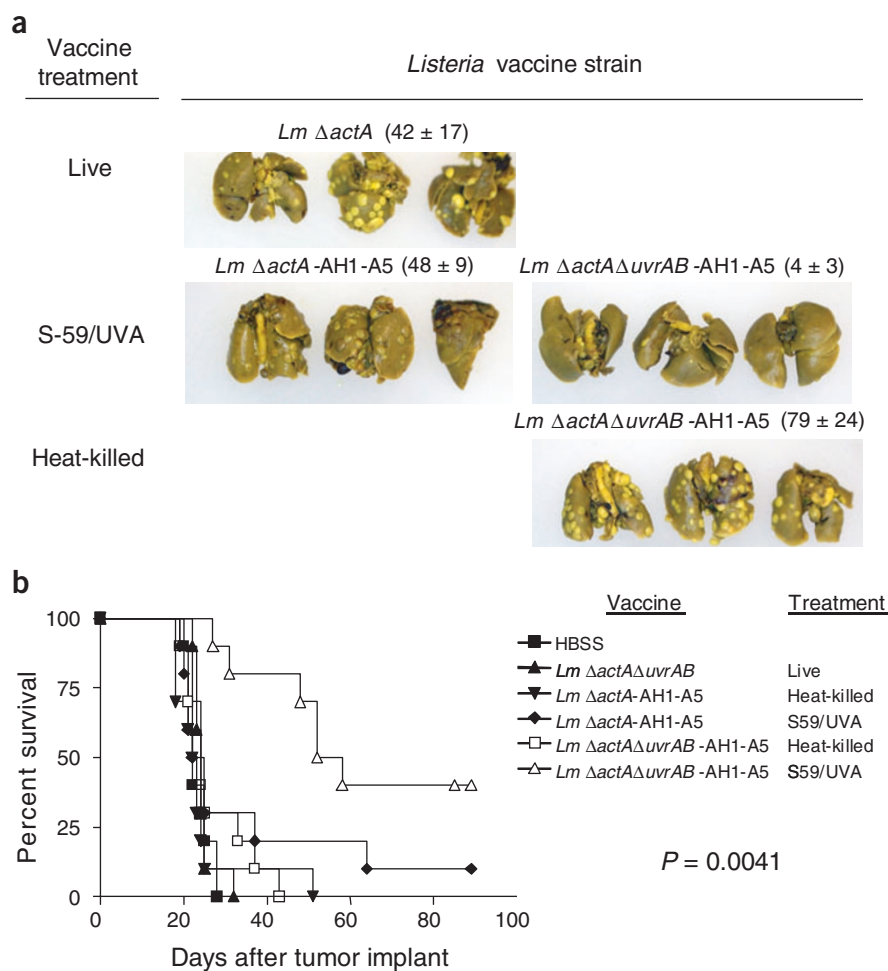


**Figure 4** Nucleotide excision repair mutation confers therapeutic efficacy of S-59/UVA *Lm ΔactAΔuvrAB*-AH1-A5 vaccines in tumor-bearing animals. (a) Lung tumor metastases 20 d after CT26 tumor cell seeding. (b) Survival; mice were killed when moribund.  $n = 10$  per group ( $P = 0.0041$ ; one-way ANOVA).

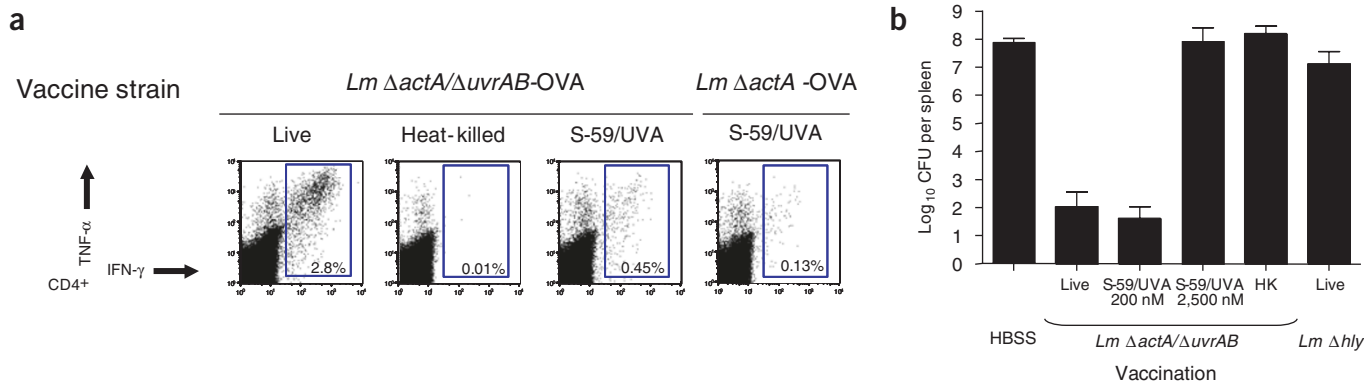


**Figure 5** S-59/UVA *Lm ΔactA/ΔuvrAB* vaccines protect immunized mice against wild-type *L. monocytogenes* challenge. **(a)** Splenic LLO<sub>190-201</sub>-specific CD4<sup>+</sup> T-cell responses from C57BL/6 mice 7 d after a single immunization with the indicated vaccines. **(b)** CFU per spleen from mice challenged with two times LD<sub>50</sub> wild-type *L. monocytogenes* 90 d after a prime-boost immunization regimen with the indicated vaccines. HK, heat-killed. Bacterial levels for three individual mice and the mean for each experiment are shown (one-way ANOVA,  $P = 0.0273$ ; Kruskal-Wallis nonparametric test with Dunn post test).

repair genes would not augment the immunogenicity of the KBMA vaccine by increasing psoralen sensitivity. Notably, higher psoralen concentrations were required to inactivate nucleotide excision repair mutant bacteria when at mid-log phase of growth (data not shown). We hypothesize that this observation resulted from an average chromosome number per bacteria in the mid-log phase cultures that exceeded one, thus facilitating recA-mediated homologous recombination repair. In turn, vaccines prepared under these conditions were poorly immunogenic (data not shown).

Formation of bacterial chains by S-59/UVA *Lm ΔactA/ΔuvrAB* but not its parental S-59/UVA *Lm ΔactA* strain after incubation in culture broth provided evidence of the capacity to synthesize macromolecules, including proteins and cell-wall constituents, and strongly distinguished the potential metabolic activity of the two S-59/UVA-treated bacterial populations. Chaining of S-59/UVA *Lm ΔactA/ΔuvrAB* is similar to the phenotype observed with certain topoisomerase mutants, in which chromosomes are not resolved after replication, producing chains of anucleate cells<sup>25</sup>, and it suggests that chromosomes after photochemical treatment are physically constrained by psoralen crosslinks, preventing cell division of nucleotide excision repair mutants.

Photochemically inactivated *Lm ΔactA/ΔuvrAB*-based vaccines may prove to be a useful tool for *ex vivo* DC-based therapies. Immature DCs efficiently take up *L. monocytogenes*, and in response undergo activation and maturation<sup>26,27</sup>. Here, we used S-59/UVA *Lm ΔactA/ΔuvrAB-OVA* vaccines to activate, mature and load a heterologous encoded antigen onto DCs, which resulted in direct MHC class I presentation *in vitro*, and primed a potent CD8<sup>+</sup> T-cell response in vaccinated mice. This approach avoids the complications related to using live bacteria in mammalian cell culture, limits the use of expensive cytokines and DC maturation reagents, and obviates the need for peptide loading. Although we have not yet compared the relative potency between recombinant S-59/UVA *Lm ΔactA/ΔuvrAB*-based and peptide-loaded DC vaccines, whole antigens can be expressed by recombinant *L. monocytogenes*-based vaccines, offering the theoretical advantage of application to individuals with diverse MHC haplotypes and without requiring knowledge of specific immunogenic epitopes.

Psoralen-inactivated nucleotide excision repair mutant analogues of commonly studied biodefense agents, such as *Bacillus anthracis* (the causative agent of anthrax), *Yersinia pestis* (the causative agent of plague) and *Francisella tularensis* (the causative agent of tularemia) could be derived from attenuated organisms in which toxins are geneti-

cally inactivated. We constructed a *B. anthracis* (Sterne) nucleotide excision repair mutant and showed its increased sensitivity to psoralen inactivation that was similar to *Lm ΔuvrAB* (data not shown). This work is based on the hypothesis that combining psoralen inactivation and metabolic activity within the context of an appropriately attenuated whole *B. anthracis* organism will result in a vaccine with greater potency that induces immune responses targeted at multiple bacterial antigens, as compared to the licensed anthrax vaccine adsorbed<sup>28</sup>. Continued studies will be a valuable test of whether this vaccine approach can be applied to understanding infection, like with *B. anthracis*, a circumstance under which humoral immunity is an essential component of immunological protection<sup>29</sup>.

Much literature exists showing the potency of *L. monocytogenes*-based vaccines in animal models for infectious disease or cancer, in both prophylactic and therapeutic settings<sup>30-36</sup>. But its role as a food-borne pathogen has hindered development and testing in humans. We have reported previously on a unique live-attenuated *L. monocytogenes* vaccine platform deleted of two virulence determinants, *actA* and *inlB*, which retains the immunogenicity of wild-type *L. monocytogenes* but is attenuated 1,000-fold in mouse virulence<sup>30</sup>. Photochemical treatment of *L. monocytogenes* nucleotide excision repair mutants represents an additional vaccine strategy for *L. monocytogenes*-based platforms, and may have application for treatment or prevention of diseases having a risk-benefit profile not appropriate for live attenuated vaccines.

## METHODS

**Bacterial strains and virus.** All *L. monocytogenes* strains were derived from the wild-type *L. monocytogenes* strain DP-L4056 (ref. 36). We generated *L. monocytogenes* strains and *B. anthracis* (Sterne) with *uvrAB* in-frame deletion by splice-overlap extension PCR and allelic exchange using established methods<sup>38,39</sup>. We used the pPL2 integration vector to construct recombinant *L. monocytogenes* strains containing a single copy of OVA and AH1-A5/OVA integrated in the bacterial genome<sup>30,37</sup>. Vaccine stocks were prepared from mid-log phase *L. monocytogenes* formulated in a mixture of 8% DMSO and PBS and stored at -80 °C. The parent and recombinant (rVV-OVA) vaccinia viruses were provided by N. Restifo (National Cancer Institute), and were grown and titered on Vero cells.

**S-59 psoralen/UVA inactivation of bacteria and metabolic activity.** We grew *L. monocytogenes* or *B. anthracis* (Sterne) in brain-heart infusion broth (Difco) at 37 °C to an OD<sub>600</sub> of 0.5 or 0.3, respectively, and we added S-59 psoralen directly to the cultures for 1 h. We transferred bacterial cultures to culture plates and UVA irradiated them at a dose of 6 or 6.5 J/cm<sup>2</sup> (FX1019 irradiation device, Baxter Fenwal), respectively. We formulated psoralen-inactivated bacteria and stored

them as described above for live bacteria. We assessed metabolic activity of live or S-59/UVA *L. monocytogenes* by autoradiography of secreted bacterial proteins separated by electrophoresis and labeled with  $^{35}\text{S}$ -methionine for 30 min after incubation for 30 min in methionine-depleted medium.

**Psoralen adduct frequency.** We determined psoralen adduct frequency by using  $^{14}\text{C}$  labeled S-59 psoralen for photochemical inactivation, according to the concentrations listed in Table 1. After photochemical treatment, we isolated genomic DNA as described<sup>40</sup>. We determined the adduct frequency (defined as the base-pair interval between psoralen adducts) by dividing the calculated DNA genomes by the S-59 psoralen molecules, determined from the DNA concentration, the radioactivity of each sample, and specific activity of  $^{14}\text{C}$  S-59 psoralen. Table 1 is representative of three independent experiments.

**Fluorescence microscopy.** We infected DC2.4 cells grown on coverslips with *L. monocytogenes* for 30 min at 37 °C at a multiplicity of infection of 10. We removed extracellular bacteria by washing with PBS and incubated infected cells for 5 h at 37 °C with 50 µg/ml gentamicin to prevent growth of extracellular bacteria. We fixed cells with 3.5% formaldehyde, stained them with *L. monocytogenes*-specific rabbit antibody (Difco), and visualized with FITC-labeled rabbit-specific goat antibody (Vector Laboratories). We detected actin using phalloidin-rhodamine (Molecular Probes) and mounted coverslips using ProLong Gold Anti-Fade containing DAPI (Molecular Probes). For assessment of bacterial morphology, we added psoralen-inactivated *L. monocytogenes* vaccines to brain-heart infusion broth media, incubated them at 37° C for the indicated period and spotted aliquots of cultures onto poly-L-lysine coverslips; we fixed bacteria, stained them with antibody and mounted them as described above.

**Mice and immunizations.** We treated 6–8-week-old female Balb/c or C57BL/6 mice (Charles River Laboratories) according to US National Institutes of Health guidelines. All protocols requiring animal experimentation received prior approval from the Cerus Animal Care and Use Committee. All vaccinations for immunogenicity, protection and tumor studies were by intravenous injection using the following doses (three mice per group, unless otherwise indicated): live *L. monocytogenes* (all strains except *Lm Dhly*),  $1 \times 10^7$  CFU; live *Lm Dhly*,  $1 \times 10^8$  CFU; heat-killed *L. monocytogenes*,  $1 \times 10^8$  infectious units; and S-59/UVA *L. monocytogenes*,  $1 \times 10^8$  IU.

**Dendritic cells.** We prepared DCs from whole bone marrow of C57BL/6 mice using high GM-CSF concentrations (20 ng/ml mouse GM-CSF; R&D Systems)<sup>41</sup>. On day 10 after plating, we verified nonadherent cells phenotypically to be myeloid DCs (CD11<sup>ch1</sup>). For immunization, bone marrow-derived DCs (CD11<sup>ch1</sup>) were incubated for 1 h with *L. monocytogenes* vaccines, washed and then  $4 \times 10^6$  infected bone marrow-derived DCs were given intravenously to C57BL/6 mice.

**B3Z T-cell hybridoma activation.** B3Z is a *lacZ*-inducible CD8<sup>+</sup> T-cell hybridoma specific for the OVA<sub>257–264</sub> (SIINFEKL) epitope presented on the mouse H-2K<sup>b</sup> class I molecule<sup>42</sup>. We cocultured  $1 \times 10^5$  DC2.4 cells infected with *L. monocytogenes* as described for fluorescent microscopy studies with B3Z cells at a ratio of 1:1 in flat-bottom 96-well plates overnight in the presence of 50 µg/ml gentamicin. We added CPRG substrate and we determined absorbance at  $\lambda = 450$  nm after 2 h. B3Z activation of DC2.4 cells infected with heat-killed *Lm*-OVA was not observed (data not shown).

**Peptides.** Peptides for *in vitro* assays were synthesized commercially (SynPep). We measured OVA-specific CD8<sup>+</sup> T cells with the H-2K<sup>b</sup>-restricted epitope SIINFEKL<sup>14</sup>. We detected *L. monocytogenes*-specific CD4<sup>+</sup> T-cell immunity with the LLO<sub>190–201</sub> epitope (NEKYAQAYPNVS)<sup>43</sup>. We assessed Gp70-specific immunity using the endogenous H-2L<sup>d</sup>-restricted epitope AH1 (SPSYVYHQF) and the altered peptide ligand AH1-A5 (SPSYAYHQF)<sup>22</sup>.

**Cytokine flow cytometry.** We determined the frequency of IFN- $\gamma$ - and tumor necrosis factor (TNF)- $\alpha$ -secreting CD4<sup>+</sup> and CD8<sup>+</sup> T lymphocytes specific for OVA, gp70, LLO from the pooled spleens of three mice per experimental group by cytokine flow cytometry as described previously<sup>30</sup>. We stained cells for cell-surface markers using antibody to CD4-fluorescein isothiocyanate (RM4-5; eBioscience) and antibody to CD8 $\alpha$ -peridinin chlorophyll protein (53-6.7;

BD Pharmingen). We fixed cells in 2% paraformaldehyde, permeabilized them with Perm/Wash buffer (BD Pharmingen), and incubated them with antibody to IFN- $\gamma$ -allophycocyanin (XMG1.2; eBioscience) and antibody to TNF- $\alpha$ -phycoerythrin (MP6-XT22; eBioscience). Samples were acquired on a FACSCalibur flow cytometer and data analyzed using FloJo software (Treestar).

**Vaccinia virus protection studies.** We gave C57BL/6 mice prime and boost vaccinations separated by 14 d with *L. monocytogenes* strains expressing OVA, and 30 d later we challenged mice intraperitoneally with  $5 \times 10^6$  plaque-forming units (PFU) of rVV-OVA. We evaluated protection by measuring viral titer in the ovaries 5 d after virus challenge as described<sup>44</sup>. Mice immunized with S-59/UVA *Lm  $\Delta$ actA/ $\Delta$ uvrAB*-OVA were not protected against challenge with parental vaccinia virus (data not shown).

**Tumor studies.** We intravenously implanted Balb/c mice with  $2 \times 10^5$  CT26 cells. We randomized mice 3 d later (ten animals per group) and vaccinated them. For enumeration of tumor nodules, we harvested lungs from mice 20 d after tumor-cell seeding, fixed them in Bouin fluid and photographed them. For survival studies, mice were killed when they started to show any signs of stress or labored breathing.

***L. monocytogenes* protection studies.** To assess protective immunity, we vaccinated C57BL/6 mice on days 0 and 14 with the indicated strains, and challenged them 90 d after vaccination with twice the LD<sub>50</sub> of wild-type *L. monocytogenes* ( $1 \times 10^5$  CFU), and we measured CFU in spleen 3 d later in organ homogenates as described previously<sup>45</sup>.

**Statistical analysis.** Differences in protection against rVV-OVA or *L. monocytogenes* challenges were determined by the Kruskal-Wallis nonparametric test with Dunn post test. Kaplan-Meier tumor survival curves were compared by the Mantel-Haenszel log-rank test. A *P* value of  $\leq 0.05$  was considered to be statistically significant. Unless otherwise indicated, all experiments were conducted at least twice.

*Note: Supplementary information is available on the Nature Medicine website.*

#### ACKNOWLEDGMENTS

We wish to thank D. Pardoll, J. Skoble, P. Lauer and A. North for their discussions, suggestions and critical review of this manuscript, and J. Cox for his suggestion of the KBMA acronym.

#### COMPETING INTERESTS STATEMENT

The authors declare competing financial interests (see the *Nature Medicine* website for details).

Received 10 February; accepted 22 June 2005

Published online at <http://www.nature.com/naturemedicine/>

- Rappuoli, R. From Pasteur to genomics: progress and challenges in infectious diseases. *Nat. Med.* **10**, 1177–1185 (2004).
- Wollowitz, S. Fundamentals of the psoralen-based Helinx technology for inactivation of infectious pathogens and leukocytes in platelets and plasma. *Semin. Hematol.* **38** 4 Suppl. 11, 4–11 (2001).
- Sancar, A. & Sancar, G.B. DNA repair enzymes. *Ann. Rev. Biochem.* **57**, 29–67 (1988).
- Unanue, E.R. Studies in listeriosis show the strong symbiosis between the innate cellular system and the T-cell response. *Immunol. Rev.* **158**, 11–25 (1997).
- Harty, J.T., Twinnereim, A.R. & White, D.W. CD8<sup>+</sup> T cell effector mechanisms in resistance to infection. *Ann. Rev. Immunol.* **18**, 275–308 (2000).
- Pamer, E.G. Immune responses to *Listeria monocytogenes*. *Nat. Rev. Immunol.* **4**, 812–823 (2004).
- Brunst, L.M., Portnoy, D.A. & Unanue, E.R. Presentation of *Listeria monocytogenes* to CD8<sup>+</sup> T cells requires secretion of hemolysin and intracellular bacterial growth. *J. Immunol.* **145**, 3540–3546 (1990).
- Portnoy, D.A., Auerbuch, V. & Glomski, I.J. The cell biology of *Listeria monocytogenes* infection: the intersection of bacterial pathogenesis and cell-mediated immunity. *J. Cell. Biol.* **158**, 409–414 (2002).
- O’Riordan, M., Yi, C.H., Gonzales, R., Lee, K.D. & Portnoy, D.A. Innate recognition of bacteria by a macrophage cytosolic surveillance pathway. *Proc. Natl. Acad. Sci. USA* **99**, 13861–13866 (2002).
- O’Connell, R.M. *et al.* Type I interferon production enhances susceptibility to *Listeria monocytogenes* infection. *J. Exp. Med.* **200**, 437–445 (2004).
- Carrero, J.A., Calderon, B. & Unanue, E.R. Type I interferon sensitizes lymphocytes to apoptosis and reduces resistance to *Listeria* infection. *J. Exp. Med.* **200**, 535–540

- (2004).
12. Auerbuch, V., Brockstedt, D.G., Meyer-Morse, N., O'Riordan, M. & Portnoy, D.A. Mice lacking the type I interferon receptor are resistant to *Listeria monocytogenes*. *J. Exp. Med.* **200**, 527–533 (2004).
  13. Lauvau, G. *et al.* Priming of memory but not effector CD8 T cells by a killed bacterial vaccine. *Science* **294**, 1735–1739 (2001).
  14. Brockstedt, D.G. *et al.* Induction of immunity to antigens expressed by recombinant adeno-associated virus depends on the route of administration. *Clin. Immunol.* **92**, 67–75 (1999).
  15. Janion, C. Some aspects of the SOS response system—a critical survey. *Acta Biochim. Pol.* **48**, 599–610 (2001).
  16. Berche, P., Gaillard, J.L. & Sansonetti, P.J. Intracellular growth of *Listeria monocytogenes* as a prerequisite for *in vivo* induction of T cell-mediated immunity. *J. Immunol.* **138**, 2266–2271 (1987).
  17. Shen, Z., Reznikoff, G., Dranoff, G. & Rock, K.L. Cloned dendritic cells can present exogenous antigens on both MHC class I and class II molecules. *J. Immunol.* **158**, 2723–2730 (1997).
  18. Auerbuch, V., Loureiro, J.J., Gertler, F.B., Theriot, J.A. & Portnoy, D.A. Ena/VASP proteins contribute to *Listeria monocytogenes* pathogenesis by controlling temporal and spatial persistence of bacterial actin-based motility. *Mol. Microbiol.* **49**, 1361–1375 (2003).
  19. Harty, J.T. & Bevan, M.J. CD8<sup>+</sup> T cells specific for a single nonamer epitope of *Listeria monocytogenes* are protective *in vivo*. *J. Exp. Med.* **175**, 1531–1538 (1992).
  20. Jensen, E.R. *et al.* Recombinant *Listeria monocytogenes* vaccination eliminates papillomavirus-induced tumors and prevents papilloma formation from viral DNA. *J. Virol.* **71**, 8467–8474 (1997).
  21. Paterson, Y. & Ikonomidis, G. Recombinant *Listeria monocytogenes* cancer vaccines. *Curr. Opin. Immunol.* **5**, 664–669 (1996).
  22. Slansky, J.E. *et al.* Enhanced antigen-specific antitumor immunity with altered peptide ligands that stabilize the MHC-peptide-TCR complex. *Immunity* **13**, 529–538 (2000).
  23. Huang, A.Y. *et al.* The immunodominant major histocompatibility complex class I-restricted antigen of a murine colon tumor derives from an endogenous retroviral gene product. *Proc. Natl. Acad. Sci. USA* **93**, 9730–9735 (1996).
  24. Shedlock, D.J. & Shen, H. Requirement for CD4 T cell help in generating functional CD8 T cell memory. *Science* **300**, 337–339 (2003).
  25. Sawitzke, J.A. & Austin, S. Suppression of chromosome segregation defects of *Escherichia coli* muk mutants by mutations in topoisomerase I. *Proc. Natl. Acad. Sci. USA* **97**, 1671–1676 (2000).
  26. Kolb-Maurer, A. *et al.* *Listeria monocytogenes*-infected human dendritic cells: uptake and host cell response. *Infection and Immunity* **68**, 3680–3688 (2000).
  27. Kolb-Maurer, A. *et al.* Production of IL-12 and IL-18 in human dendritic cells upon infection by *Listeria monocytogenes*. *FEMS Immunol. Med. Microbiol.* **35**, 255–262 (2003).
  28. Case Report: Use of anthrax vaccine in the United States: recommendations of the advisory committee on immunization practices. *Clinical Toxicology* **39**, 85–100 (2001).
  29. Reuveny, S. *et al.* Search for correlates of protective immunity conferred by anthrax vaccine. *Infect. Immun.* **69**, 2888–2893 (2001).
  30. Brockstedt, D.G. *et al.* *Listeria*-based cancer vaccines that segregate immunogenicity from toxicity. *Proc. Natl. Acad. Sci. USA* **101**, 13832–13837 (2004).
  31. Starks, H. *et al.* *Listeria monocytogenes* as a vaccine vector: virulence attenuation or existing antivector immunity does not diminish therapeutic efficacy. *J. Immunol.* **173**, 420–427 (2004).
  32. Gunn, G.R. *et al.* Two *Listeria monocytogenes* vaccine vectors that express different molecular forms of human papilloma virus-16 (HPV-16) E7 induce qualitatively different T cell immunity that correlates with their ability to induce regression of established tumors immortalized by HPV-16<sup>1</sup>. *J. Immunol.* **167**, 6471–6479 (2001).
  33. Pan, Z.-K., Ikonomidis, G., Pardoll, D. & Paterson, Y. Regression of established tumors in mice mediated by the oral administration of a recombinant *Listeria monocytogenes* vaccine. *Cancer Research* **55**, 4776–4779 (1995).
  34. Shen, H. *et al.* Recombinant *Listeria monocytogenes* as a live vaccine vehicle for the induction of protective anti-viral cell-mediated immunity. *Proc. Natl. Acad. Sci. USA* **92**, 3987–3991 (1995).
  35. Liao, L.M. *et al.* Tumor immunity within the central nervous system stimulated by recombinant *Listeria monocytogenes* vaccination. *Cancer Res.* **62**, 2287–2293 (2002).
  36. Peters, C., Peng, X., Douven, D., Pan, Z.-K. & Paterson, Y. The induction of HIV gag-specific CD8<sup>+</sup> T cells in the spleen and gut-associated lymphoid tissue by parenteral or mucosal immunization with recombinant *Listeria monocytogenes* HIV gag. *J. Immunol.* **170**, 5176–5187 (2003).
  37. Lauer, P., Chow, M.Y., Loessner, M.J., Portnoy, D.A. & Calendar, R. Construction, characterization, and use of two *Listeria monocytogenes* site-specific phage integration vectors. *J. Bacteriol.* **184**, 4177–4178 (2002).
  38. Horton, R.M., Cai, Z.L., Ho, S.N. & Pease, L.R. Gene splicing by overlap extension: tailor-made genes using the polymerase chain reaction. *Biotechniques* **8**, 528–535 (1990).
  39. Camilli, A., Tilney, L.G. & Portnoy, D.A. Dual roles of plcA in *Listeria monocytogenes* pathogenesis. *Mol. Microbiol.* **8**, 143–157 (1993).
  40. Wilson, C. Preparation of genomic DNA from bacteria. in *Current Protocols in Molecular Biology* (eds. Ausubel, F.M. *et al.*) 2.4.1–2.4.5 (John Wiley & Sons, Hoboken, New Jersey, 1997).
  41. Lutz, M.B. *et al.* An advanced culture method for generating large quantities of highly pure dendritic cells from mouse bone marrow. *J. Immunol. Methods* **223**, 77–92 (1999).
  42. Malarkannan, S. & Shastri, N. Generation of antigen-specific, lacZ-inducible T-cell hybrids. *Methods Mol. Biol.* **156**, 1–8 (2000).
  43. Geginat, G., Schenk, S., Skoberne, M., Goebel, W. & Hof, H. A novel approach of direct *ex vivo* epitope mapping identifies dominant and subdominant CD4 and CD8 T cell epitopes from *Listeria monocytogenes*. *J. Immunol.* **166**, 1877–1884 (2001).
  44. Alexander-Miller, M.A., Leggett, G.R. & Berzofsky, J.A. Selective expansion of high- or low-avidity cytotoxic T lymphocytes and efficacy for adoptive immunotherapy. *Proc. Natl. Acad. Sci. USA* **93**, 4102–4107 (1996).
  45. Busch, D.H.C. Animal model for infection with *Listeria monocytogenes*. *Current Protocols in Immunology* Vol. 3. (eds. Coligan, J.E., Kruisbeek, A.M., Margulies, D.H., Shevach, E.M. & Strober, W.) 19.9.1–19.9.9 (John Wiley & Sons, Hoboken, New Jersey, 2000).
  46. Lenz, L.L. & Portnoy, D.A. Identification of a second *Listeria* secA gene associated with protein secretion and the rough phenotype. *Mol. Microbiol.* **45**, 1043–1056 (2002).